STAR Results from the RHIC Beam Energy Scan

HUI WANG FOR THE STAR COLLABORATION

RM 1-174, Building 510A, Brookhaven National Laboratory, Upton, NY, 11973

The Beam Energy Scan Program is launched by RHIC to study the QCD phase diagram. The goal is to explore the possible QCD phase boundary and search for possible QCD critical point. In 2010 and 2011, experiments collected data at $\sqrt{s_{NN}}$=7.7,11.5,19.6,27,39 and 62.4 GeV, covering a wide range of baryon chemical potential from μ_B 420 to 70 MeV. In this presentation, we will report some latest results of the Beam Energy Scan Program from the STAR collaboration.

1. Introduction

Current results from RHIC and LHC indicate the existence of a deconfined Quark Gluon Plasma (QGP) phase at high energy in A+A collisions. One major challenge, however, is to understand the structure of the QCD phase diagram. If the temperature is high and μ_B is relatively small, both lattice QCD and experimental data indicate this transition from hadronic matter to Quark Gluon Plasma is an analytical transition (cross-over) [1], while some theoretical calculations predict that the transition at lower temperatures and high μ_B is a first order phase transition [2]. If a phase transition exists at higher μ_B, with a cross-over at $\mu_B = 0$, the phase transition would end in a critical point at finite μ_B. However, due to the difficulty of lattice QCD calculations at finite μ_B, accurate predictions of the critical point location are still lacking [3]. Therefore it falls to experiment to search for traces of the existence of the critical point of QCD.

To further explore the QCD phase diagram, a Beam Energy Scan (BES) proposal was made by the STAR Collaboration [4], which aims to search for the turn-off of QGP signatures, signals for first order phase transition and the critical point. The first phase of the BES program was started in 2010 with collisions recorded at $\sqrt{s_{NN}} = 7.7$, 11.5, 39 GeV and finished in 2011 with collisions at $\sqrt{s_{NN}}$=19.6 and 27 GeV. In this paper, a few selected results from the STAR BES program will be discussed.

2. Search for Turn-off of QGP Signatures

2.1. the Balance Function

The balance functions, which measure the correlation between the opposite sign charge pairs, are sensitive to the mechanisms of charge formation and the subsequent relative diffusion of the balancing charges [5]. Due to conservation laws like electric charge conservation, particles and their antiparticles are pair produced and correlated initially in coordinate space, if a delayed hadronization occurs, the lower temperature and less expansion and diffusion will result in a narrower charge balance function [5]. It has been reported that the balance function for $\Delta\eta$ narrows at top RHIC energies [6]. Thus the balance function could be used to probe the evolution of the system hadronization time vs. energy and search for possible turn-off of QGP at lower energies.
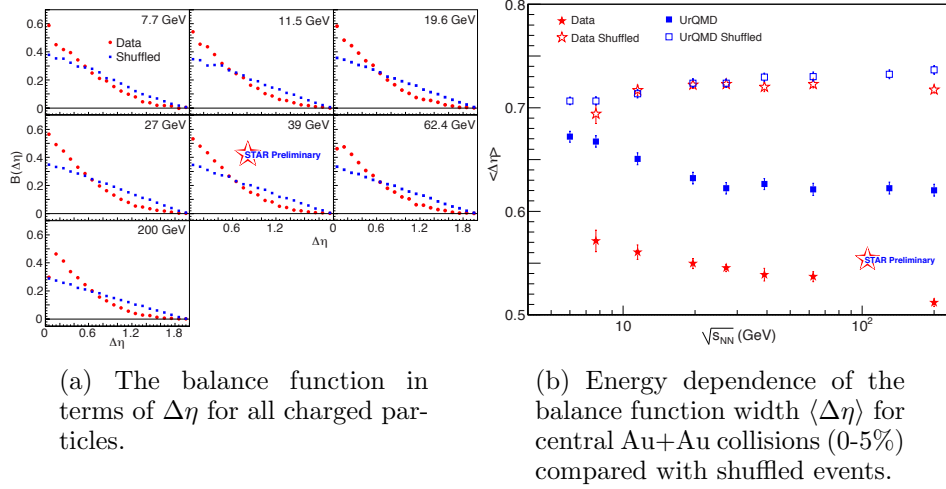

(a) The balance function in terms of $\Delta\eta$ for all charged particles.

(b) Energy dependence of the balance function width $\langle\Delta\eta\rangle$ for central Au+Au collisions (0-5%) compared with shuffled events.

Fig. 1: The balance function in terms of $\Delta\eta$ for all charged particles. Central events (0-5%) are shown here with $\sqrt{s_{\mathrm{NN}}}$ from 7.7 to 200 GeV.

For this analysis, we use all charged particles with the transverse momentum cut of $0.2 < p_t < 2.0\,\mathrm{GeV}/c$ and the pseudorapidity cut of $|\eta| < 1.0$. Figure 1a shows the balance function in terms of $\Delta\eta$ for all charged particles. The most central events (0-5%) are shown for seven incident energies. The data in the figure are the balance function results from real data corrected by subtracting the balance function calculated using mixed events. We can see that, for all the energies shown here, the balance functions from data are narrower than the ones from shuffled events. To quantify the narrowing of balance function, figure 1b shows the energy dependence of the balance func-

tion width for central Au+Au collisions. The data show a smooth decrease of $\langle \Delta \eta \rangle$ with increasing energy. UrQMD calculations predict a similar trend but over predict the observed results. Since the balance function is sensitive to the hadronization time and relative diffusion after hadronization, this decrease in balance function width could mean a longer lived QGP phase at higher energies. The UrQMD model is a hadronic model that does not have a deconfined phase transition and has little flow. This early hadronization time combined with strong interaction between final particles leads to a wider balance function in UrQMD. In the same figure, the shuffled events from both data and UrQMD show a wider balance function that slightly increases with increasing energy.

2.2. Elliptic Flow

Elliptic flow is the second harmonic coefficient of the Fourier expansion

$$\frac{dN}{d\phi} \propto 1 + 2 \sum_{n \geq 1} v_n \cos\left[n(\phi - \Psi_n)\right] , \tag{1}$$

where ϕ is the azimuthal angle of the particles and Ψ is the reconstructed event plane azimuthal angle. Elliptic flow would be generated by the initial pressure gradient created by non-central heavy ion collisions. One major line of evidence that a deconfined quark gluon plasma is produced in Au+Au collisions at $\sqrt{s_{NN}} = 200$ GeV is the number-of-constituent quark (NCQ) scaling of v_2 versus transverse momentum p_T for hadrons at intermediate p_T (2 to 5 GeV/c) [7, 8]. Deviations from such a scaling at lower beam energies could be an indication for the absence of the deconfined phase [9].

Figure 2 shows the differences in v_2 between particles X (p, Λ, Ξ^-, π^+, K^+) and corresponding anti-particles $\overline{X}$ ($\bar{p}$, $\overline{\Lambda}$, $\overline{\Xi}^+$, π^-, K^-) with $\sqrt{s_{NN}}$. Larger v_2 values are found for particles than for antiparticles, except for pions for which the opposite ordering is observed. The difference increases with decreasing beam energy and is larger for baryons compared to mesons [10].

As discussed previously, the universal NCQ scaling of v_2 at $\sqrt{s_{NN}} = 200$ GeV suggests strongly interacting partonic matter is produced. The observed difference in v_2 at lower beam energies demonstrates that this common NCQ scaling of particles and anti-particles splits. Such a breaking of the NCQ scaling could indicate increased contributions from hadronic interactions in the system evolution with decreasing beam energy, or could be related to the larger values of μ_B.
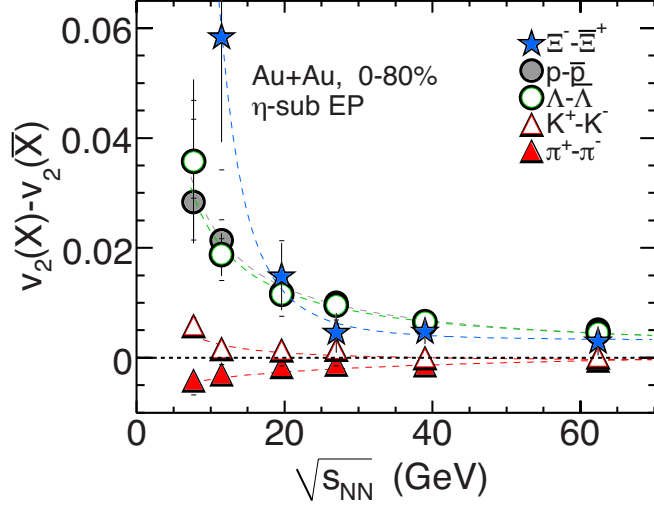
Fig. 2: The difference in v_2 between particles (X) and their corresponding anti-particles ($\overline{X}$) (see legend) as a function of $\sqrt{s_{NN}}$ for 0–80% central Au+Au collisions. The dashed lines in the plot are fits with a power-law function [10].

3. Search for Critical Point

3.1. Particle Ratio Fluctuations

The energy dependence of particle-ratio fluctuations is also an interesting topic. Enhanced fluctuations are one of the possible signatures of a phase transition near a critical point [11]. The observable ν_{dyn} for kaons and pions can be written as

$$\nu_{dyn,K\pi} = \frac{<K(K-1)>}{<K>^2} + \frac{<\pi(\pi-1)>}{<\pi>^2} - \frac{2<K\pi>}{<K><\pi>} , \qquad (2)$$

Figure 3a shows the $\nu_{dyn,K\pi}$ results for 7.7–200 GeV [12, 13, 14]. STAR results are approximately independent of collision energy. This disagrees with NA49's results, which show a strong increase with decreasing incident energy. The same figure also shows model calculations. The points labeled STAR UrQMD represent UrQMD calculations with STAR acceptance cuts, which show little energy dependence and over predict the magnitude of the data. The HSD model predicts increased fluctuations at low energies and agrees with the NA49 measurements at the lowest energies but over predict

the data at higher energies. None of the models presented here can fully describe the incident energy dependence of the data.
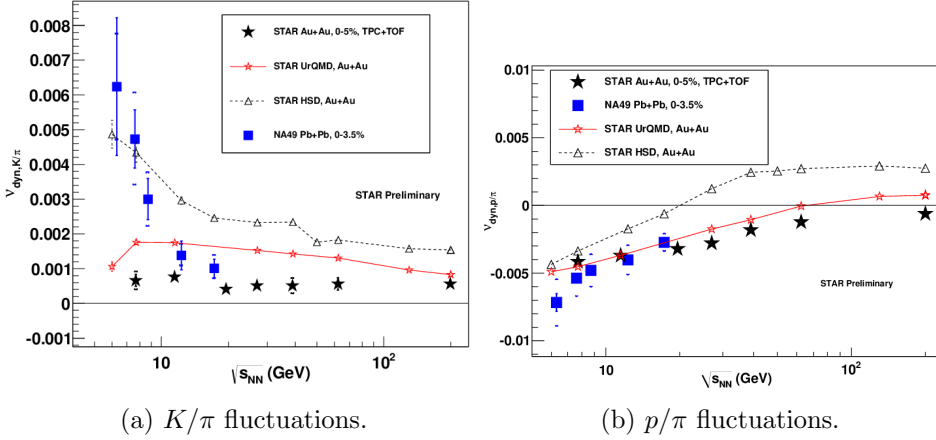

(a) K/π fluctuations. (b) p/π fluctuations.

Fig. 3: Energy dependence of K/π and p/π fluctuations expressed as $\nu_{\mathrm{dyn},p/\pi}$. Only central events are shown here (0-5% for STAR Au+Au collisions, 0–3.5% for NA49 Pb+Pb collisions). UrQMD and HSD calculations are also shown.

Unlike the results for K/π fluctuations, the results for p/π fluctuations are affected by resonance correlations (e.g. Δ, Λ, Σ all decay to p, π). These correlations increase the cross-correlation terms of ν_{dyn} and produce a negative ν_{dyn} value. Figure 3b shows the incident energy dependence of $\nu_{\mathrm{dyn},p\pi}$. The STAR and NA49 results for p/π fluctuations show good agreement. They are both negative and increase with increasing collision energy. The UrQMD model describes the data well at SPS energies, which supports the resonance correlations interpretation because UrQMD is a hadronic transport model. However, UrQMD becomes positive and over predicts the data at higher energies.

p/K fluctuations, which are related to baryon-strangeness correlations, can be used as a tool to study the deconfinement phase transition. Figure 4a shows the incident energy dependence of $\nu_{\mathrm{dyn},Kp}$ results. The STAR data show a smooth decrease with decreasing collision energy and disagree with NA49 data at 7.7 GeV. Further study is still needed to understand the differences between the two experiments. A UrQMD calculation with the STAR acceptance filter is also shown in the same figure. UrQMD always over predicts fluctuations and becomes positive at high collision energies. The HSD model always predicts positive ν_{dyn} results.

(a) Energy dependence of p/K fluctuations. UrQMD and HSD calculations are also shown.

(b) $\sqrt{\langle \Delta p_{t,i} \Delta p_{t,j} \rangle}/\langle\langle p_t \rangle\rangle$ as a function of incident energy. UrQMD calculations are also shown in the same figure.
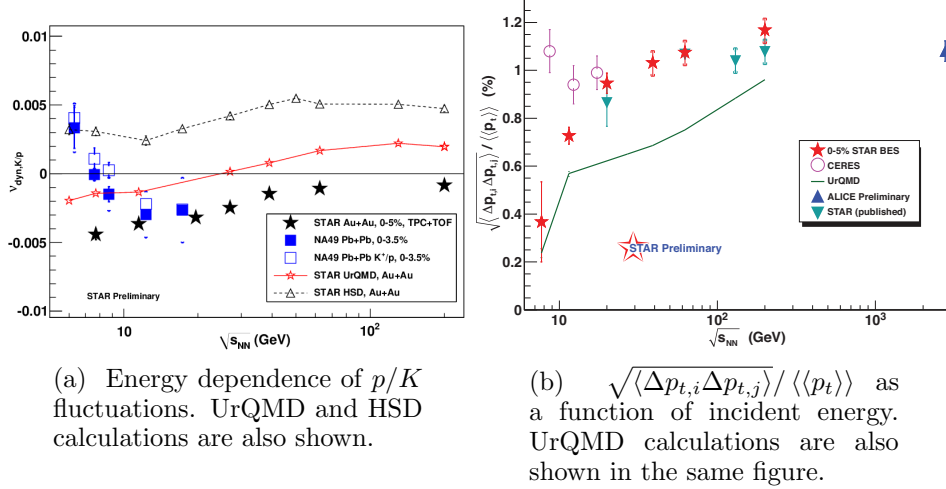
Fig. 4: Energy dependence of p/K fluctuations and p_t Fluctuations. Only central events are shown here.

3.2. p_t Fluctuations

The p_t fluctuations could also serve as a signal for the QCD critical point or the occurrence of thermalization and collectivity [15, 16]. One observable for the event-by-event two particle momentum correlation is defined [17] as

$$\langle \Delta p_{t,i} \Delta p_{t,j} \rangle = \frac{1}{N_{\text{event}}} \sum_{k=1}^{N_{\text{event}}} \frac{C_k}{N_k(N_k - 1)}, \tag{3}$$

where

$$C_k = \sum_{i=1}^{N_k} \sum_{j=1, i\neq j}^{N_k} \left(p_{t,i} - \langle\langle p_t \rangle\rangle\right)\left(p_{t,j} - \langle\langle p_t \rangle\rangle\right). \tag{4}$$

Figure 4b shows the incident energy dependence of p_t correlations. The STAR data shows a rapid increase from 7.7 to 62.4 GeV and then little energy dependence up to 2.76 TeV. UrQMD shows a similar increasing trend but under predicts the measured correlations. The CERES data deviates from STAR at lower energy. Effects due to different experimental acceptances are still under investigation.

4. Search for First Order Phase Transition

One important goal of the STAR BES program is to search for the evidence of a first order phase transition. The HBT technique can be used to

determine the freeze-out eccentricity ε_F. A non-monotonic behavior of ε_F as a function of energy could indicate a soft point in the equation of state [20]. Figure 5a shows the excitation function of the freeze-out eccentricity. The combined E895 and STAR data shows a smooth decrease of ε_F with energy. Also, the UrQMD model reproduces both E895 and STAR data. Overall, no non-monotonic behavior is observed in ε_F.

(a) Freeze-out eccentricity, ϵ_F , as a function of $\sqrt{s_{NN}}$ for data and models [19].

(b) Directed flow slope (dv_1/dy) near mid-rapidity as a function of beam energy for mid-central (10-40%) Au+Au collisions.
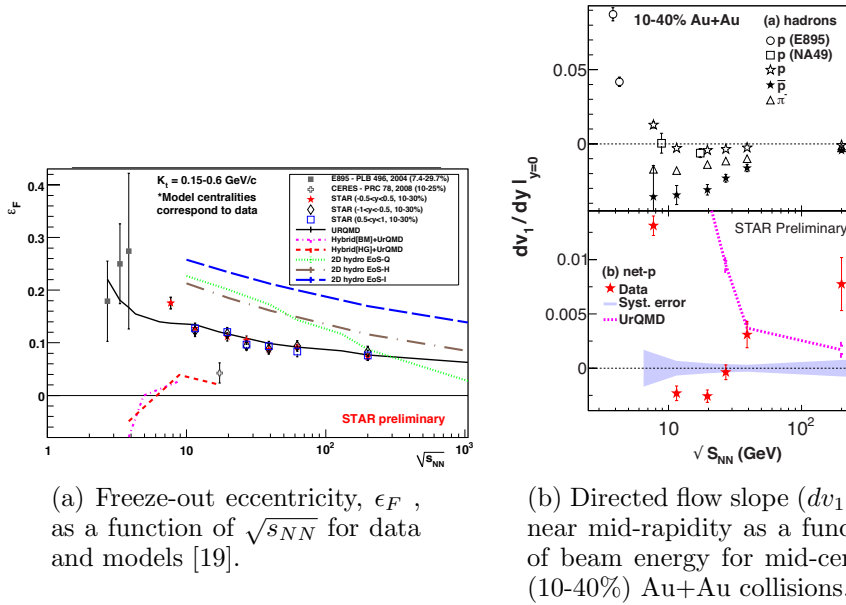
Fig. 5: Energy dependence of ϵ_F and dv_1/dy

Directed flow, which measures the "side-splash" motion of the collision products, is sensitive to the equation of state (EOS) and hence can be considered a first order phase transition signal [18]. Figure 5b shows the energy dependence of directed flow slope (dv_1/dy) near mid-rapidity for 10-40% central Au+Au collisions [21]. The v_1 slope for net protons is calculated via the relation $F_p = rF_{\bar{p}} + (1 - r)F_{\text{net-p}}$, where r is the observed ratio of antiprotons to protons among the analyzed tracks. The net proton v_1 slope changes sign twice and shows a minimum at $\sqrt{s_{NN}} =10$ to 20 GeV. This result is qualitatively different from UrQMD and AMPT transport models, which both predict a monotonic trend throughout $\sqrt{s_{NN}} =7.7$ to 200 GeV [21]. Further studies are needed to understand the current results and their implications for the Equation of State.

5. Summary

We have presented some of the latest results from the STAR BES Phase I program. Most results show a smooth change vs. incident energy. We do see significant differences in particle and anti-particle v_2, which indicates the breaking of the NCQ scaling. A possible minimum at $\sqrt{s_{NN}} =$10–20 GeV is also observed for the net proton v_1 slope. More statistics are needed to confirm a few other interesting observables such as higher moments of net-protons distributions and ϕ-meson v_2. We are looking forward to the BES Phase II program with STAR iTPC upgrade and fixed-target mode [22].

References

[1] Y. Aoki *et al.*, Nature **443**, 675 (2006).

[2] S. Ejiri, Phys. Rev. D **78**, 074507 (2008).

[3] M.A. Stephanov PoS LAT2006:024 (2006).

[4] M.M. Aggarwal *et al.* (STAR Collaboration), arXiv:1007.2613v1.

[5] S.A. Bass, P. Danielewicz, and S. Pratt, Phys. Rev. Lett. **85**, 2689 (2000).

[6] B.I. Abelev *et al.* (STAR Collaboration), Phys. Rev. C **82**, 024905 (2010).

[7] J. Adams *et al.* (STAR Collaboration), Phys. Rev. Lett. **95**, 122301 (2005).

[8] B.I. Abelev *et al.* (STAR Collaboration), Phys. Rev. C **75**, 054906 (2007).

[9] M.M. Aggarwal *et al.* (STAR Collaboration), arXiv:1007.2613 [nucl-ex].

[10] L. Adamczyk *et al.* (STAR Collaboration), Phys. Rev. Lett. **110**, 142301 (2013).

[11] V. Koch, arXiv:0810.2520 [nucl-th].

[12] C. Alt *et al.*, Phys. Rev. C **79**, 044910 (2009).

[13] J. Adams *et al.* (STAR Collaboration), Phys. Rev. Lett. **103**, 092301 (2009).

[14] T.J. Tarnowsky (STAR Collaboration), arXiv:1110.2222 [nucl-ex]..

[15] M.A. Stephanov, K. Rajagopal, and E.V. Shuryak Phys. Rev. Lett. **81**, 4816 (1998).

[16] S. Gavin, Phys. Rev. Lett. **92**, 162301 (2004).

[17] J. Adams *et al.* (STAR Collaboration), Phys. Rev. C **72**, 044902 (2005).

[18] R. Snellings *et al.*, Phys. Rev. Lett. **84**, 2803 (2000); J. Brachmann *et al.*, Phys. Rev. C **61**, 024909 (2000); L.P. Csernai and D. Rohrich, Phys. Lett. B **458**, 454 (1999); H. Stoecker, Nucl. Phys. A **750**, 121 (2005).

[19] N. Shah (STAR Collaboration), arXiv:1210.5436 [nucl-ex].

[20] M. A. Lisa, E. Frodermann, G. Graef, M. Mitrovski, E. Mount, H. Petersen, and M. Bleicher, New J. Phys. **13**, 065006 (2011).

[21] Y. Pandit (STAR Collaboration), arXiv:1210.5315 [nucl-ex].

[22] RHIC Beam Use Request For Runs 13 and 14.